Simultaneous Thermoelectric and Optoelectronic Characterization of Individual Nanowires

SAND2016-8328C

George T. Wang, *Brian Swartzentruber, Qiming Li, François Léonard*
Sandia National Laboratories

Erdong Song, Julio Martinez
New Mexico State University

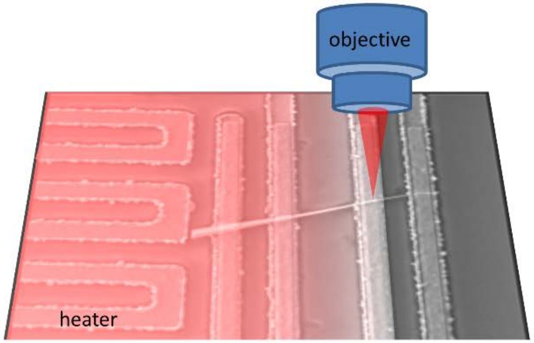

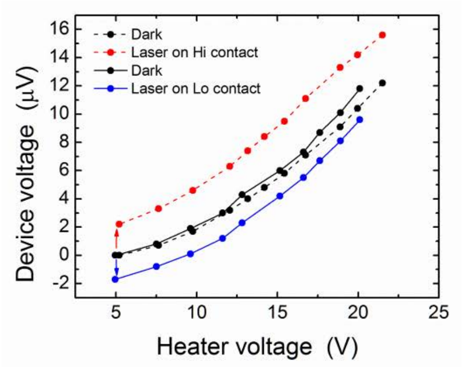

F. Léonard et al, Nano Letters **15**, 8129 (2015)

Much interest in the photoconductive properties of nanostructures from basic science & applied perspectives:

MoS$_2$ photoconductivity

(Lopez-Sanchez et al, Nat. Nanotech. 2013)

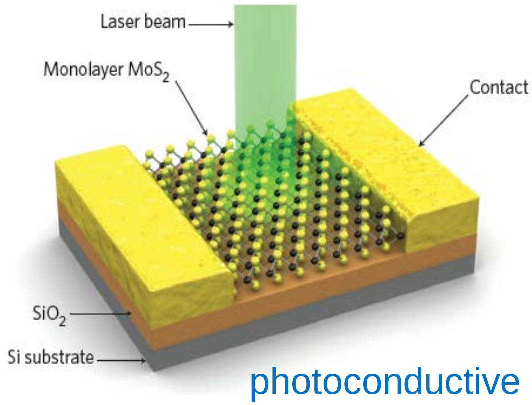

photoconductive effect

Carbon nanotube THz detector

(X. He et al., Nano Letters 2014)

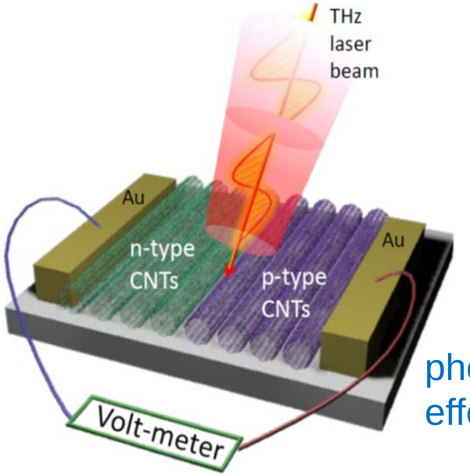

photothermoelectric effect

Graphene photodetector

(Mueller et al, Nat. Photon. 2010)

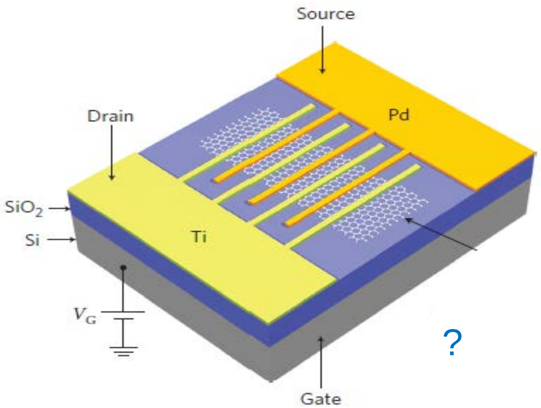

?

Nanowire solar cell

(Marianni et al., Nano Letters 2011)

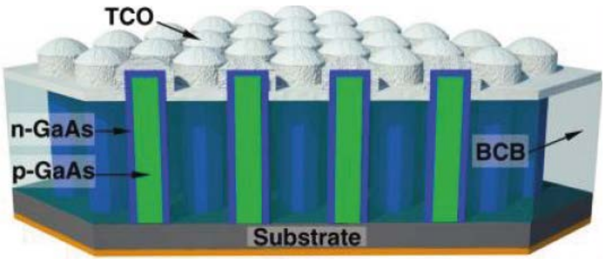

Photovoltaic effect

Several mechanisms have been proposed for the origin of the photoresponse:

- Photovoltaic
- Photoconductive
- Bolometric
- Photothermoelectric
- Photogating

We are interested in identifying which mechanisms govern the properties of specific nanostructures and nanodevices.

Nanowires based on wide bandgap materials are promising for UV photodetectors:

ZnO nanowires
Soci et al, NanoLett 2007

GaN nanowires
Lähnemann et al, NanoLett 2007

Questions:

-How do we differentiate between photocurrent mechanisms?

-Is there more than one mechanism?

Today:

-Combined optoelectronic and thermoelectric platform for nanostructures

-Application to GaN/AlGaN nanowires reveals coexistence of photoresponse mechanisms with different spatial location and temporal behavior.

Calarco et al
Nano Lett 2005

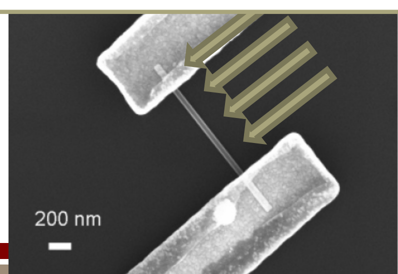

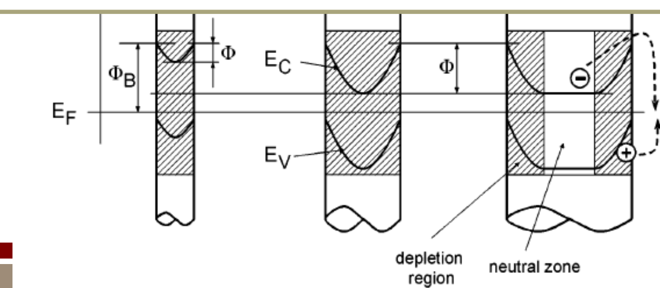

“Bottom Up” aligned GaN nanowire growth

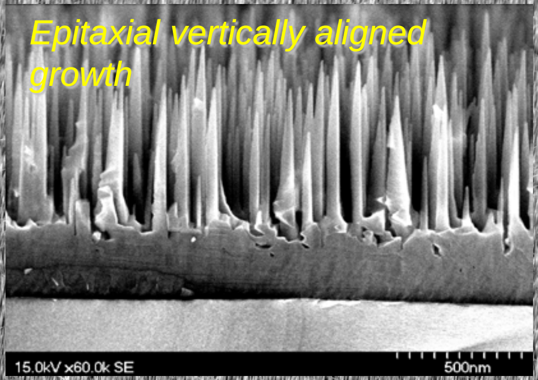

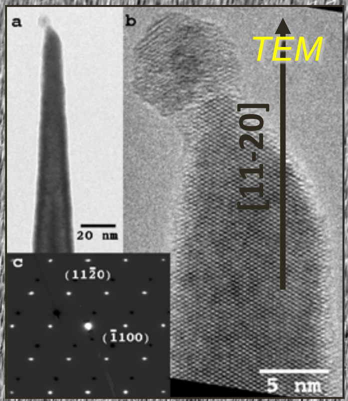

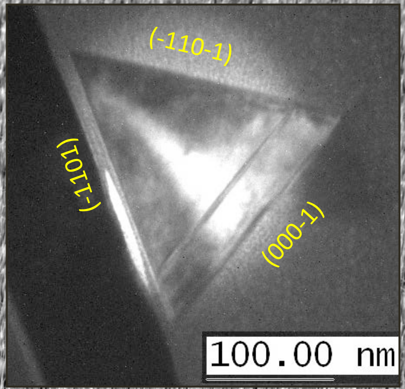

- Nanowires grown by Ni-catalyzed MOVPE/MOCVD (VLS)
- Highly-aligned vertical growth over large areas (2” r-sapphire wafer)
- Controllable densities as high as ~150 nanowires μm^{-2}
  - Q. Li, G. T. Wang, *Appl. Phys. Lett. 93, 043119* (2008)
  - Q. Li, J. R. Creighton, G.T. Wang. *J. Crys. Growth 310 3706-3709* (2008)
- Primary [11-20] growth orientation (⊥ to (11-20) *a*-plane)
- Triangular faceted -- (000-1) and equiv. (-1101) and (-110-1)
- TEM: Single crystal, dislocation free; *c*-plane stacking faults
  - G. T. Wang et al., *Nanotechnology 17 5773-5780* (2006)

George T. Wang

100 µm

Sandia - Bottom-up III-nitride nanowires

Vertically-aligned growth

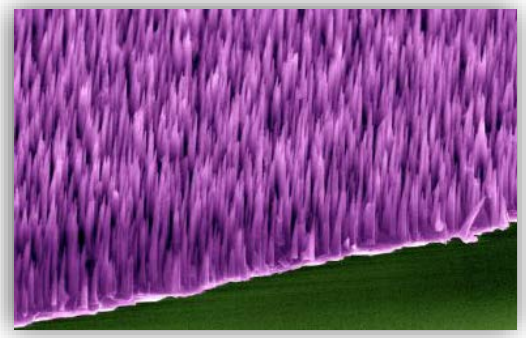

G. T. Wang et al., *Nanotechnology 17 5773-5780* (2006)
Q. Li, G. T. Wang, *Appl. Phys. Lett. 93, 043119* (2008)
Q. Li, J. R. Creighton, G.T. Wang. *J. Crys. Growth 310 3706-3709* (2008)

Nanowire-templated growth

Q. Li, Y. Lin, J.R. Creighton, J. Figiel, G.T. Wang, *Adv. Mat.*, **21** 2416–2420 (2009)

Electrical characterization

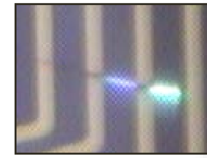

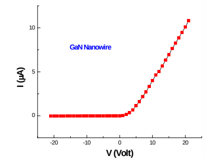

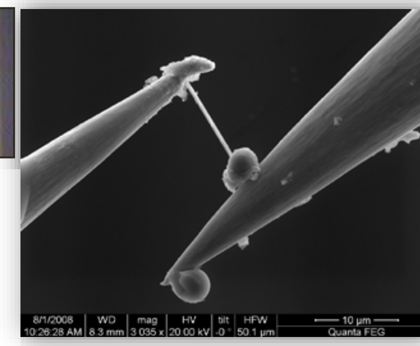

A. A. Talin, G. T. Wang, E. Lai, R. J. Anderson, *Appl. Phys. Lett.* **92** 093105 (2008)
Y. Lin, Q. Li, A. Armstrong, and G. T. Wang, *Solid State Commun.*, ***149****, 1608 (2009)*

Optical imaging and spectroscopy

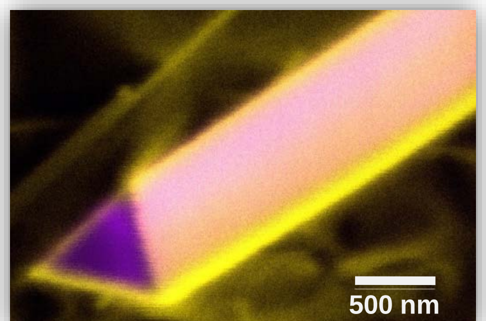

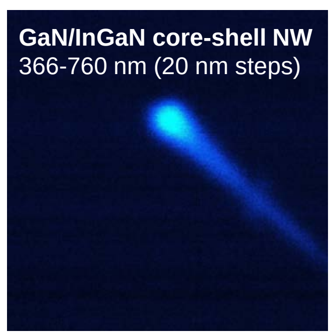

Q. Li, G. T. Wang, *Nano Lett.*, 2010, 10 (5), 1554 [GaN defect CL]
Q. M. Li, G. T. Wang, "*Appl. Phys. Lett.*, ***97***, 181107, 2010. [Gan/InGaN]
P.C. Uppadhya et al. *Semicond. Sci. Tech.* **25** 024017 (2010) [Ultrafast]
A. Armstrong, Q. Li, Y. Lin, A. A. Talin, G. T. Wang, APL **96**, 163106 (2010). [DLOS]

In-situ TEM

T. Westover et al., *Nano Lett.*, **9**, 257 (2009). [*in-situ* NW breakdown]
J. Y. Huang et al., *Nano Lett*, ***11* *(4),*** *1618* ***(2011).*** [*in-situ* nanomechanics]

Theory

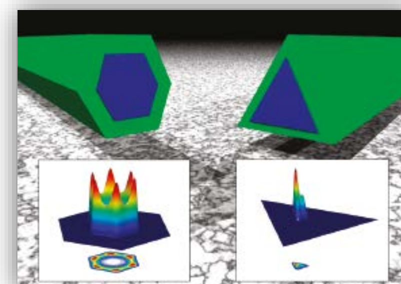

B. Wong et al., *Nano Lett* ***11* *(8)****, 3074, 2011*

GaN/AlGaN core/shell nanowires

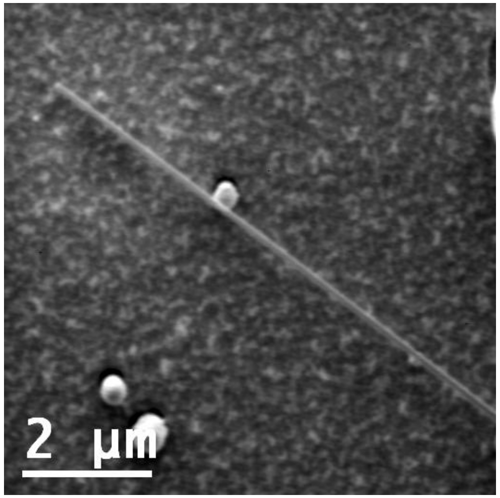

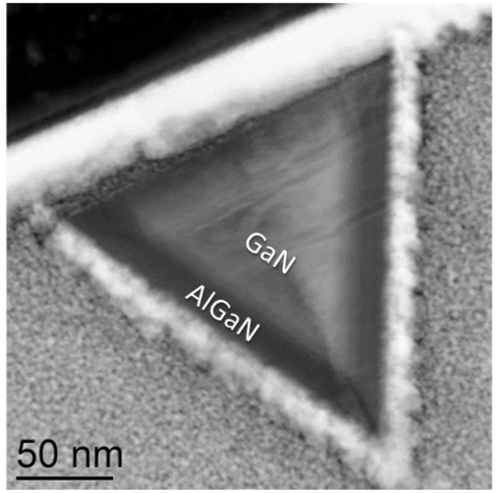

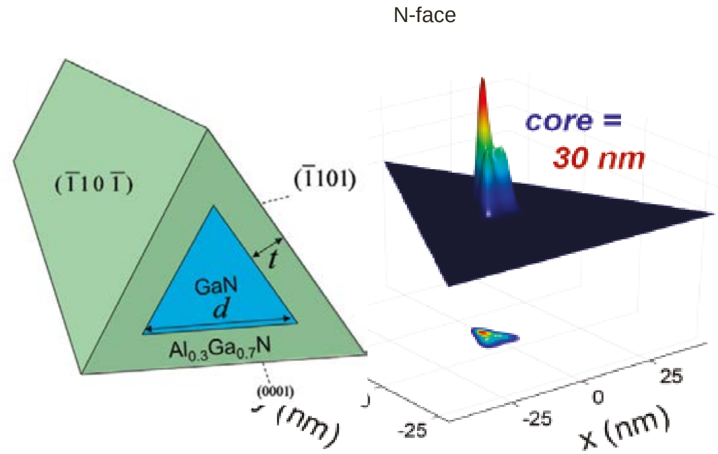

B. Wong et al., *Nano Lett* ***11 (8)***, *3074, 2011*

GaN core: 900 °C; AlGaN shell: ~1050 °C, shell thicknesses ~10 – 35 nm, Al content from ~20 – 30% (EDS), tapered ~150-250 nm widths, ~ 15 μm lengths

Previous theoretical and experimental work predicts/suggests formation of electron gas in GaN/AlGaN core-shell nanowires

- Li et al., *Nano Lett.* **6**, *1468 (2006)*

GaN/AlGaN of interest for:

- Light emitting diodes and lasers
- High speed electronics (2DEG HEMTs)
- Solar blind/UV photodetectors

Experimental Setup

Scanning Photocurrent Microscopy

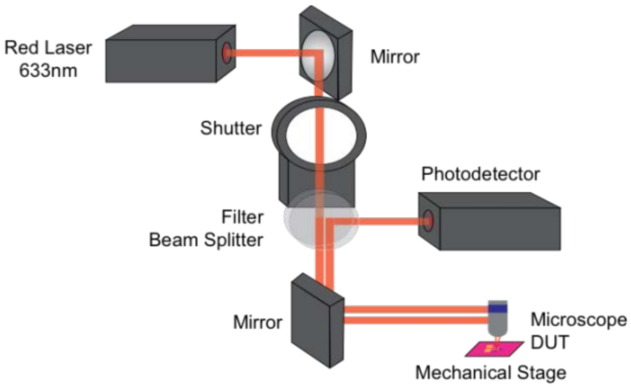

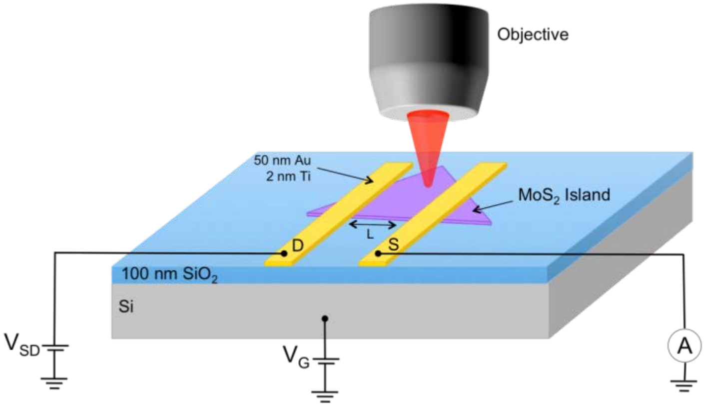

Klee et al, *Nano Letters* **15**, 2612 (2015)

Thermoelectric + SPCM Platform

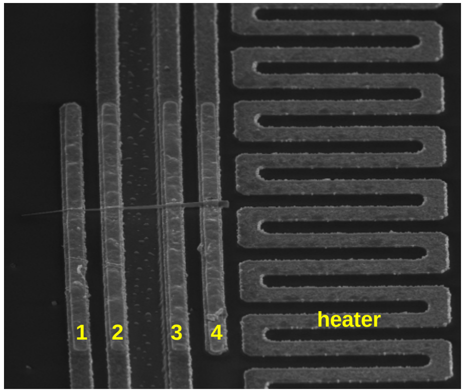

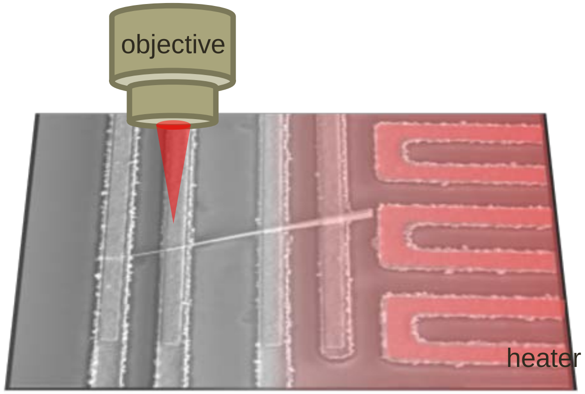

E. Song et al., *Nanotechnology*, ***27***, 015204 **(2016)**

Experimental Setup

E. Sor

Thermoelectric Properties in Core-Shell NW

Core-Shell NW thermoelectric transport

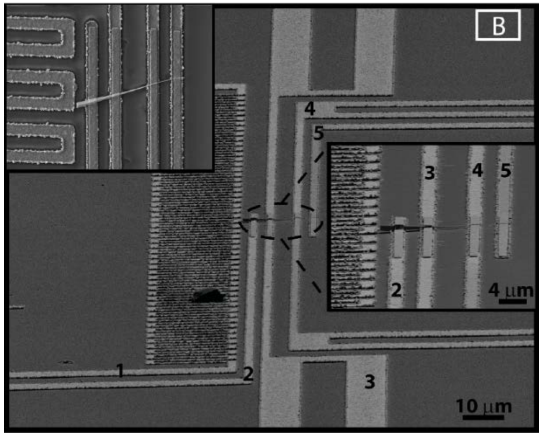

Carrier concentration

$$Z = \frac{S^2\ \sigma}{K}$$

Nanostructuring (phonon)

- All thermoelectric properties; Ohmic contacts.

Electrical Conductivity

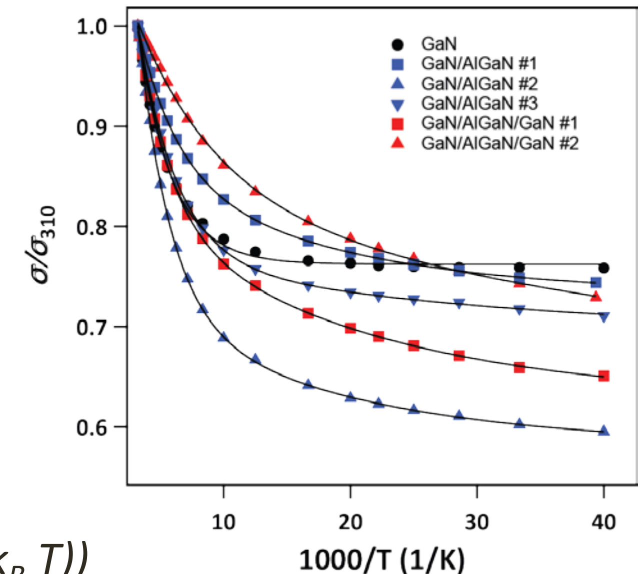

$$\sigma(T)=\sigma_0+\sigma_1 * exp(-E_{a1}/(k_B\ T))+\sigma_2 * exp(-E_{a2}/(k_B\ T))$$

	σ_0 (S/cm)	σ_1 (S/cm)	E_{a1} (meV)	σ_2 (S/cm)	E_{a2} (meV)
GaN #1	90.1 ± 0.2	90.7 ± 3.5	31.8 ± 0.9	-	-
GaN/AlGaN #1	43.4 ± 0.2	77.0 ± 0.8	34.5 ± 0.6	12.4 ± 0.5	5.4 ± 0.4
GaN/AlGaN #2	37.3 ± 0.5	36.3 ± 0.1	28.3 ± 0.0	4.6 ± 0.3	3.0 ± 0.0
GaN/AlGaN #3	78.6 ± 0.4	44.0 ± 1.1	28.1 ± 1.7	16.5 ± 1.5	5.6 ± 0.8
GaN/AlGaN/GaN #1	31.2 ± 0.2	35.3 ± 0.8	34.9 ± 1.2	10.9 ± 0.2	4.8 ± 0.4
GaN/AlGaN/GaN #2	30.6 ± 1.1	14.8 ± 0.4	13.3 ± 1.1	10.8 ± 1.0	1.4 ± 0.8

Heavily doped UID GaN

$n_{GaN} \approx 1.3\times10^{19}\ cm^{-3}$

Low activation, energy second conduction channel is present in GaN/AlGaN and GaN/AlGaN/GaN NWs

Electron and Hole Gas in Core-Shell NWs

The sign of the Seebeck coeff. indicates the type majority of carriers

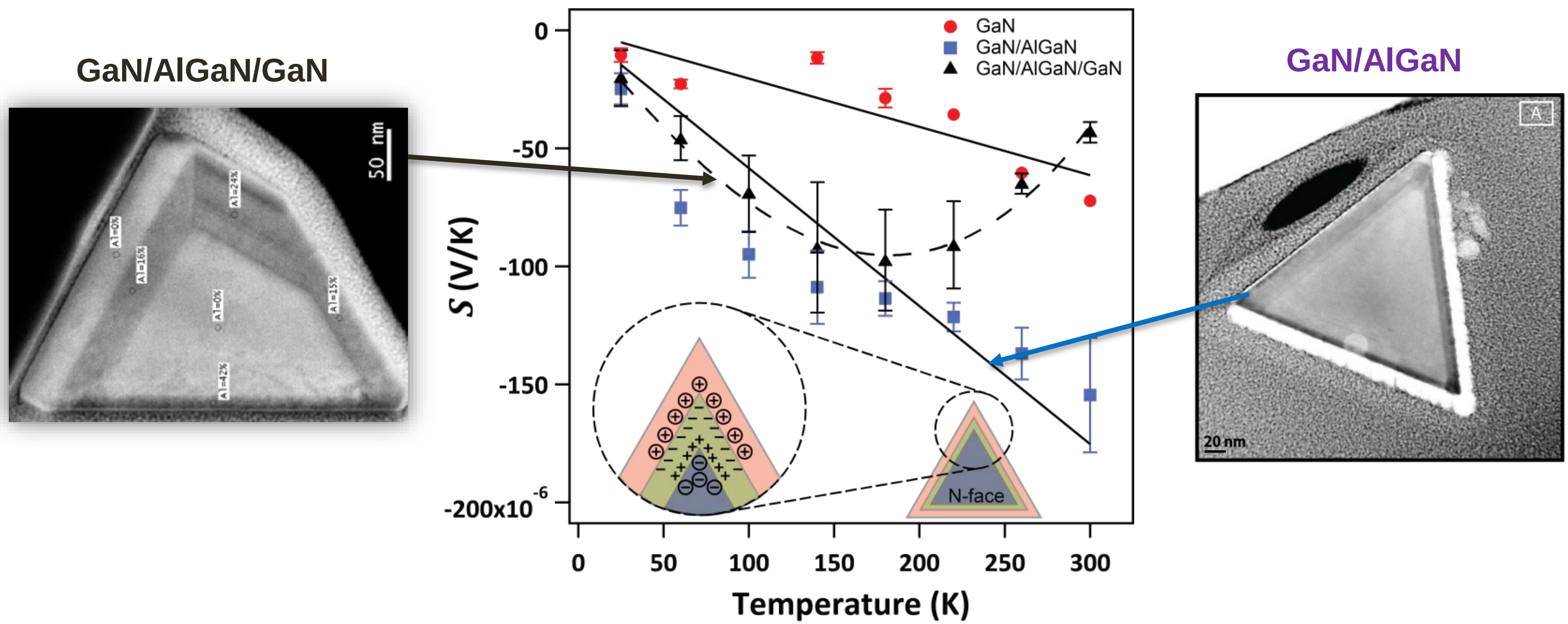

- *S* of GaN/AlGaN is 3 about times the one of GaN. Increased *S* due to possible electron gas (EG has a low thermal activation energy).
- *S* of GaN/AlGaN/GaN is the smallest. Hole gas layer in the GaN outer shell induced by electron gas layer in core.

Scanning Photocurrent Microscopy at zero bias

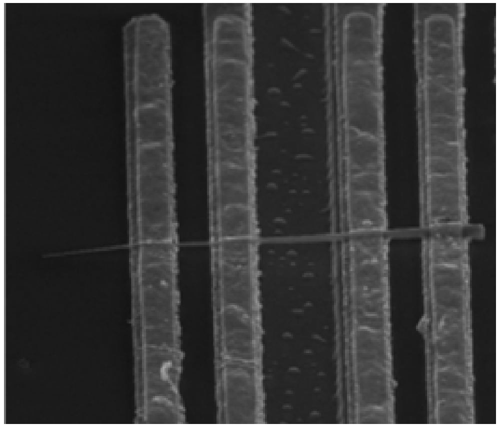

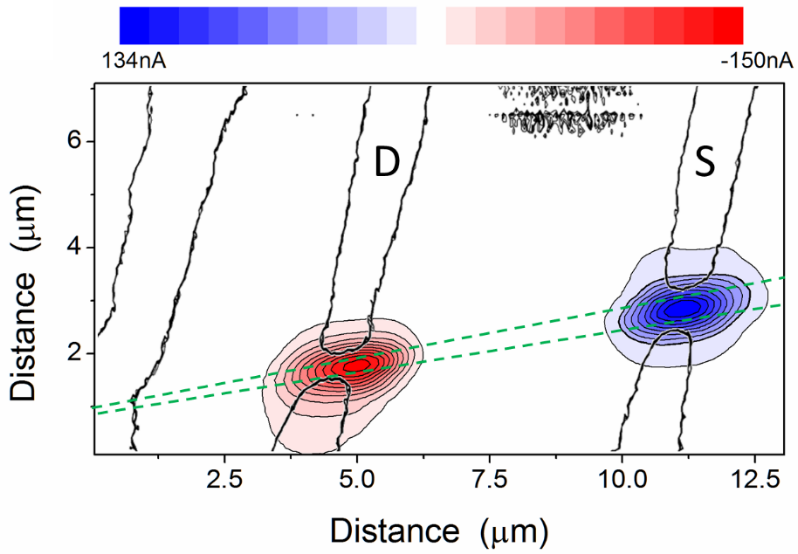

Likely candidate: photothermoelectric effect

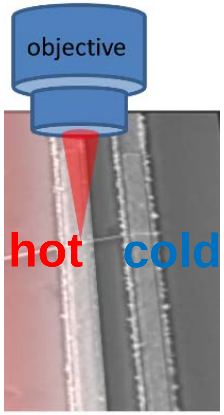

$$\Delta V = -S\Delta T$$

Thermoelectric + Optoelectronic

use the heater to generate a thermal gradient across the source and drain as in the normal thermoelectric measurement, and at the same time we focus the red laser on a particular location on the nanowire device.

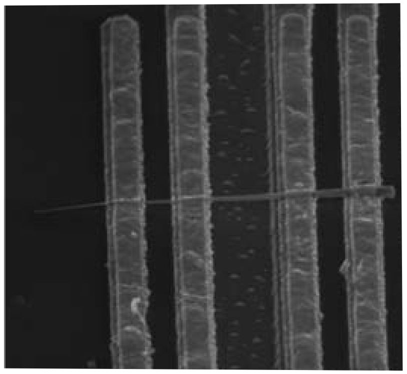

$$\Delta V = -S\Delta T$$

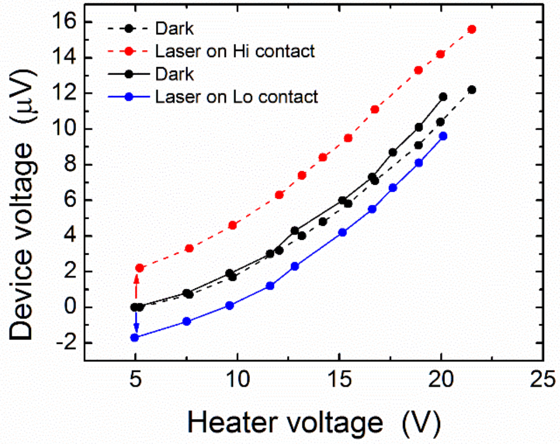

- Seebeck coefficient directly measured: -78 uV/K
- Sign of Seebeck agrees with sign of photocurrent
- V across NW depends on heater power, indicating light acting same as heat
- For illumination of the already hot (cold) electrode, the voltage increases (decreases) indicating that the light serves the same role as heat.
- Also allows extraction of temperature increase (16.5 K/mW)
- From temperature increase can extract materials properties by modeling (e.g. heat transfer coefficient ~2 × 10^8 W/m^2 K,)

F. Léonard et al, Nano Letters **15**, 8129 (2015)

What about the photogating?

- **Emerges when there is an applied source-drain bias:**

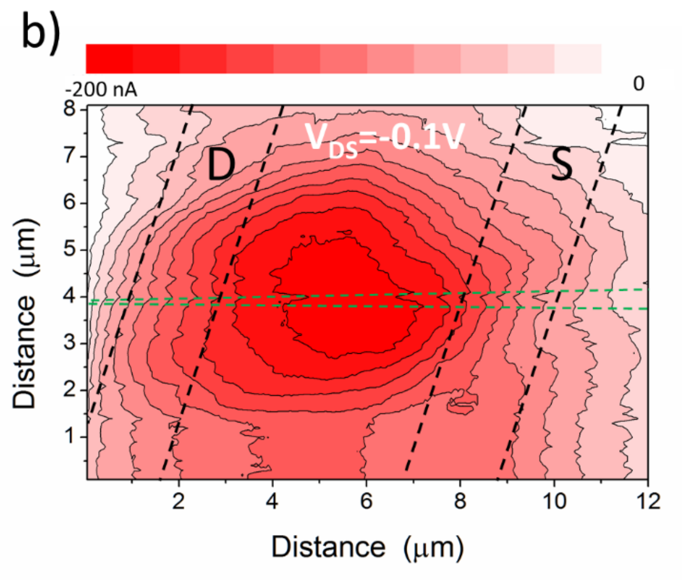

Photocurrent now appears in the channel, with only one sign.

Comparing photothermoelectric and photogating mechanisms

	Spatial location	*Power dependence*	*Temporal behavior*

Photothermoelectric

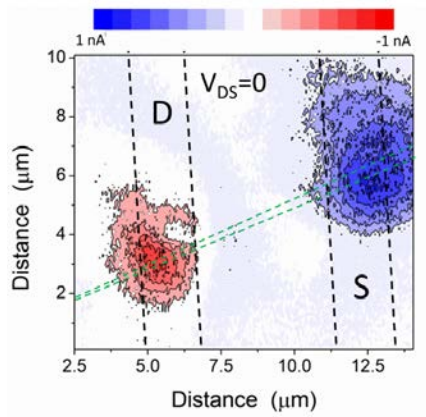

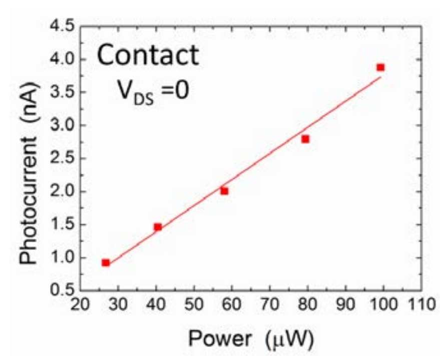

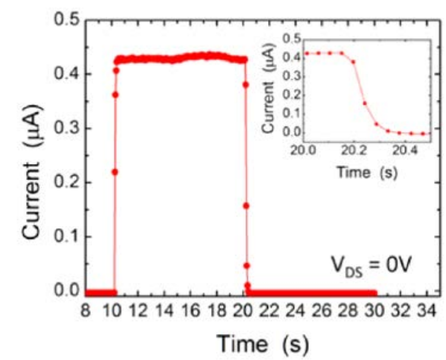

Photogating

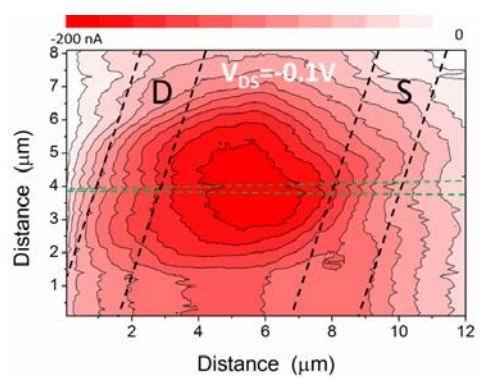

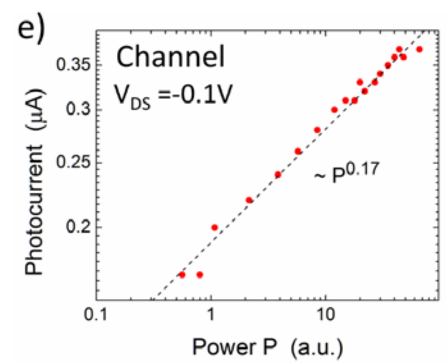

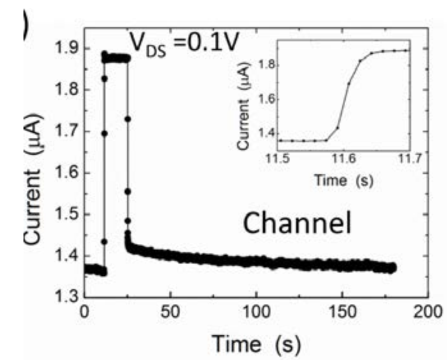

The story is not so simple: coexistence of mechanisms

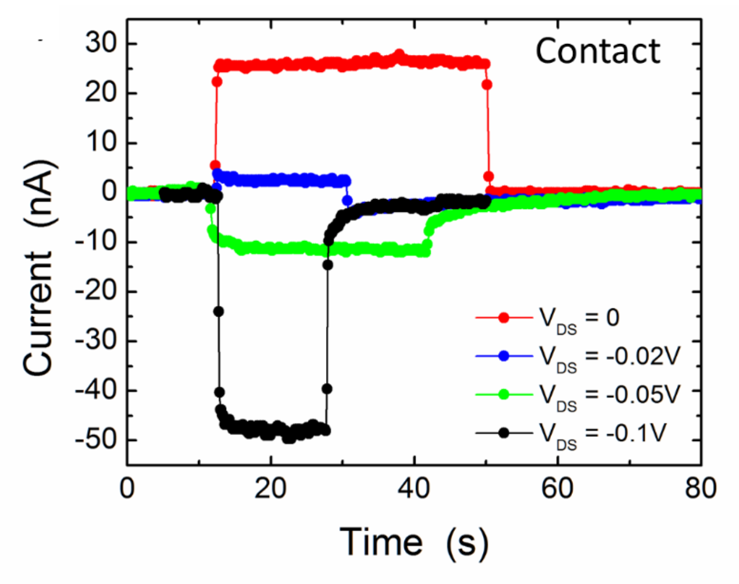

As the voltage is increased, the sign of the photocurrent at/near the contacts changes sign!

Time scale for decay shows that at low bias the photothermoelectric effect dominates, but at larger bias the photogating effect dominates.

F. Léonard et al, Nano Letters **15**, 8129 (2015)

Thanks to our sponsors:

Sandia National Laboratories is a multiprogram laboratory managed and operated by Sandia Corporation, a wholly owned subsidiary of Lockheed Martin Corporation, for the DOE's National Nuclear Safety Administration, under contract No. DE-AC-04-94AI-85000.

Backup Slides

Scanning Photocurrent Microscopy

(a) (b) (c) (d)

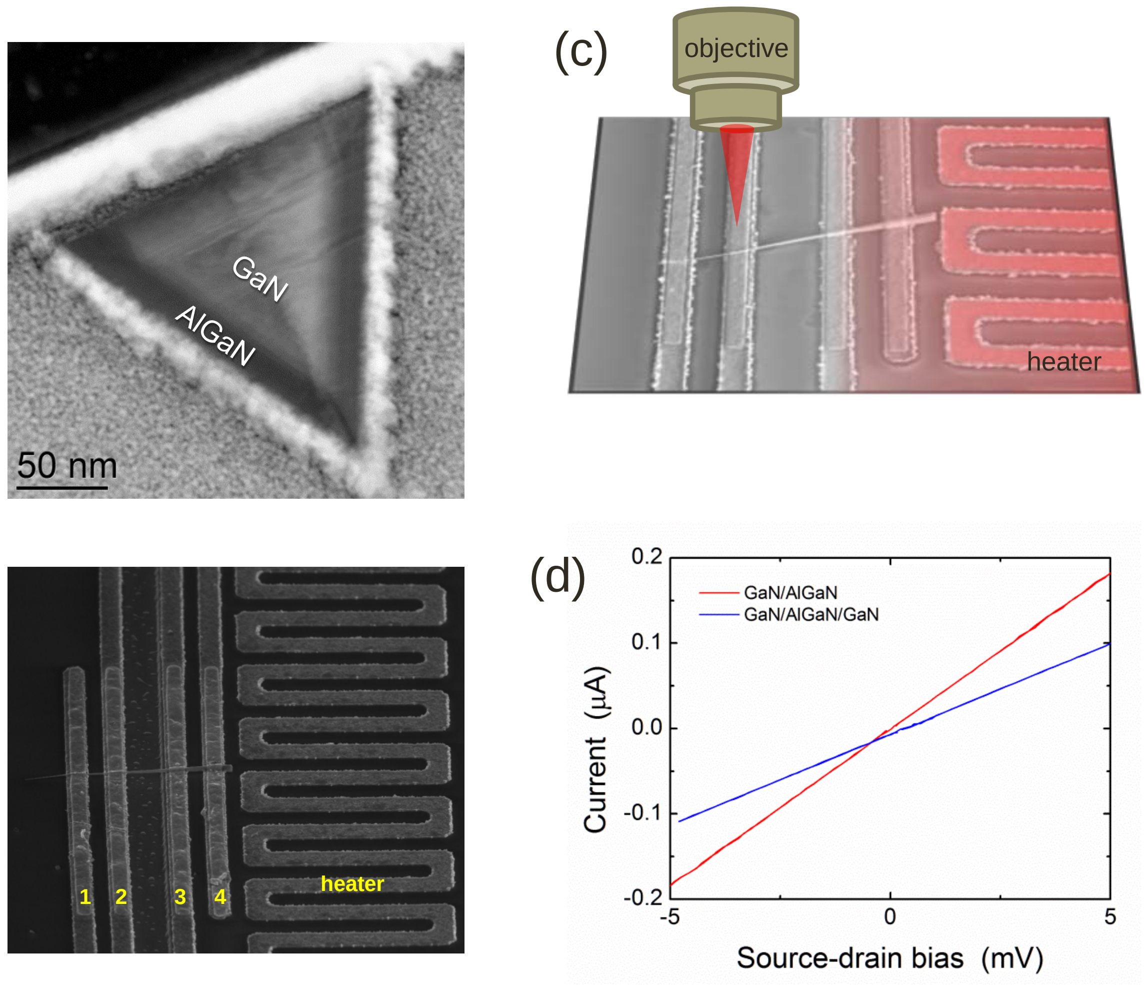

Enhanced thermoelectric transport in AlGaN/GaN nanowires

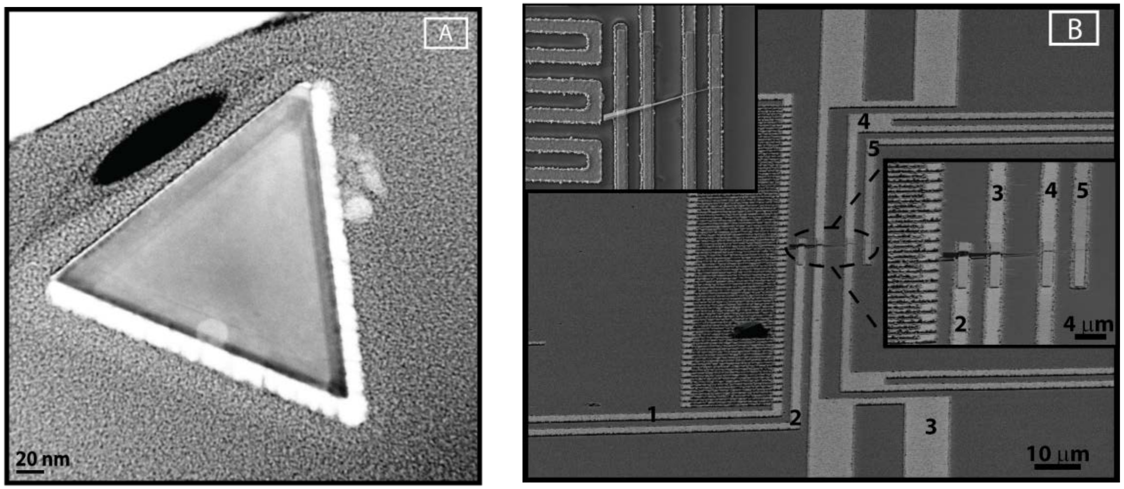

A: Cross-section STEM image of GaN/AlGaN core-shell NW. B: SEM image of our thermoelectric characterization platform. Right inset: zoom-in showing a GaN/AlGaN nanowire suspended on the 4 metal contacts. Left top inset: SEM top view of the same device measurements; lead 1 is the heater for thermoelectric voltage measurements.

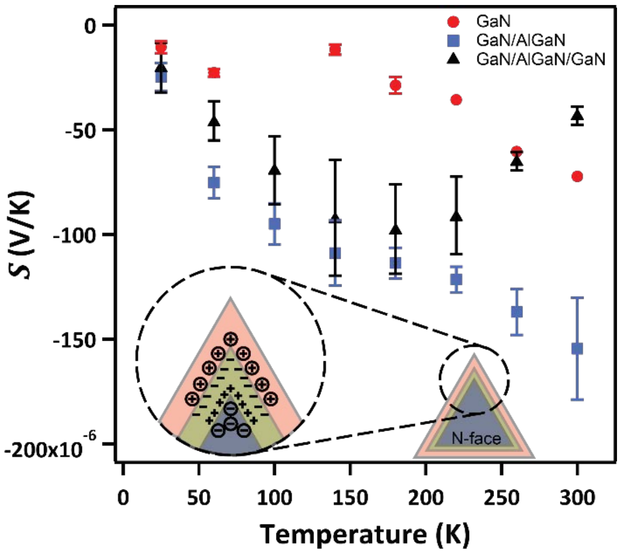

Measured Seebeck coefficient versus T.

- AlGaN/GaN core-shell NW shows greater Seebeck coefficient by > 2x vs. GaN NW
- Enhanced Seebeck coefficient may be result of electron gas channel at AlGaN/GaN interface

E. Song, Q. Li, B. Swartzentruber, W. Pan, G. T. Wang, J. A. Martinez, "Enhanced thermoelectric transport in modulation-doped GaN/AlGaN core/shell nanowires", *Nanotechnology*, ***27***, 015204 **(2016)**.

Fig. 3

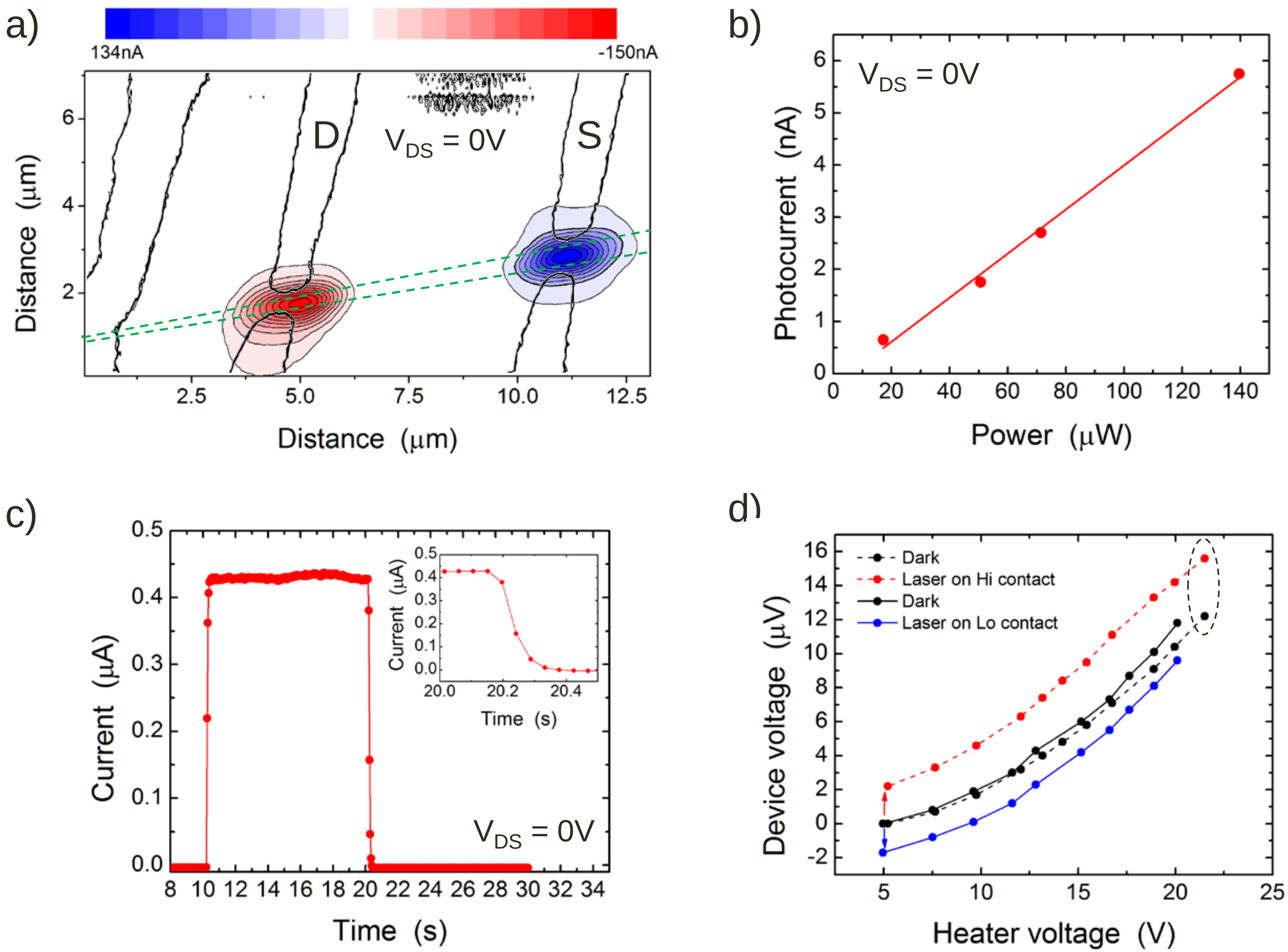

Sandia National Laboratories

Fig. 4

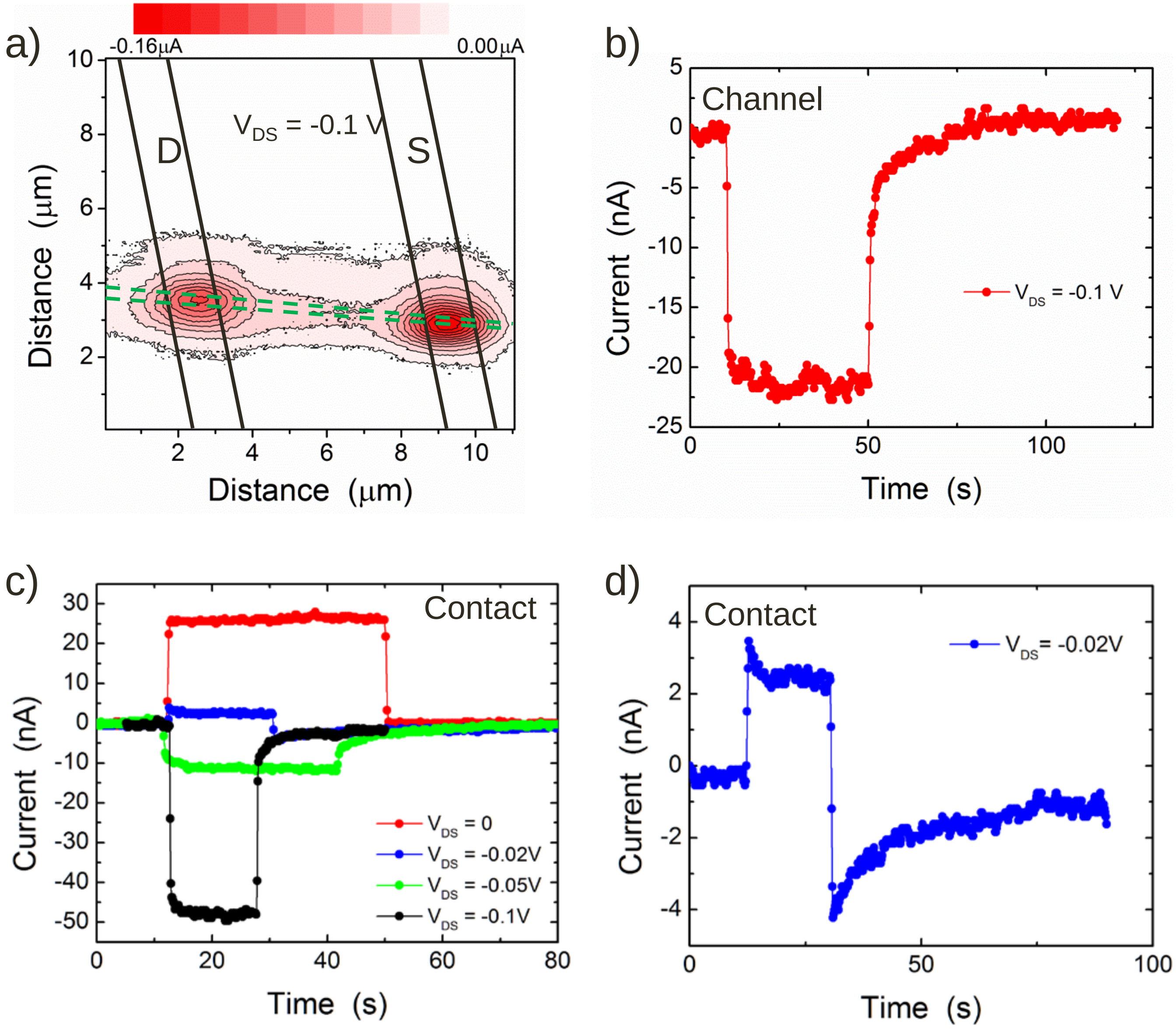
a)
-0.16μA
0.00μA
V_DS = -0.1 V
D
S
Distance (μm)
Distance (μm)
b)
Channel
V_DS = -0.1 V
Current (nA)
Time (s)
c)
Contact
V_DS = 0
V_DS = -0.02V
V_DS = -0.05V
V_DS = -0.1V
Current (nA)
Time (s)
d)
Contact
V_DS= -0.02V
Current (nA)
Time (s)